

Ultrafast Dynamics of Intersubband Excitations in a Quasi-Two-Dimensional Hole Gas

Robert A. Kaindl, Matthias Wurm, Klaus Reimann, Michael Woerner, and Thomas Elsaesser
Max-Born-Institut für Nichtlineare Optik und Kurzzeitspektroskopie, Max-Born-Straße 2A, D-12489 Berlin, Germany

Christian Miesner, Karl Brunner, and Gerhard Abstreiter
Walter-Schottky-Institut, Technische Universität München, Am Coulombwall, D-85748 Garching, Germany
(Received 13 June 2000)

We present the first study of ultrafast hole dynamics after resonant intersubband excitation in a quasi-two-dimensional semiconductor. *p*-type Si_{0.5}Ge_{0.5}/Si multiple quantum wells are studied in pump-probe experiments with 150 fs midinfrared pulses. Intersubband scattering from the second heavy-hole back to the first heavy-hole subband occurs with a time constant of 250 fs, followed by intrasubband carrier heating within 1 ps. Such processes give rise to a strong reshaping of the intersubband absorption line, which is accounted for by calculations of the subband structure, optical spectra, and hole-phonon scattering rates.

DOI: 10.1103/PhysRevLett.86.1122

PACS numbers: 78.47.+p, 71.20.-b, 73.21.-b

The quantization of electronic states in quasi-two-dimensional (2D) semiconductors creates a series of valence and conduction subbands with consecutive energy spacings below the fundamental band gap. Optical intersubband (IS) absorption promotes carriers into higher subbands and induces a sequence of microscopic interactions between the carriers and other excitations of the material on ultrashort time scales. For electrons, both theoretical calculations and ultrafast experiments have given valuable insights into fundamental processes such as the decay of coherent IS polarizations, IS relaxation by polar optical phonon scattering, thermalization, or cooling [1]. Moreover, IS transitions and electron-phonon interactions form the basis of the quantum cascade laser, a novel source of coherent midinfrared radiation [2].

In contrast, hole IS dynamics has remained largely unexplored. It is expected to differ fundamentally due to (i) the complex valence band structure, resulting in a variety of intra- and intervalence band scattering channels, and (ii) the different nature of hole-phonon interactions. Generally, the sequence of valence subbands is determined by the different confinement potentials of heavy-hole (HH), light-hole (LH), and split-off (SO) subbands, and—if existing—by built-in strain. Intervalence band absorption occurs as in the bulk [3], but IS absorption, with the dipole moment perpendicular to the quantum well layers, emerges only between valence subbands of similar character, as for HH1 → HH2 transitions. The valence subbands are characterized by a strong nonparabolicity and warping [4], which originates from the mutual admixture of their mostly *p*-like cell-periodic basis states at in-plane momenta $k_{\parallel} \neq 0$. This band mixing induces a k_{\parallel} dependence of optical IS transition frequencies and of the dipole moment [5], and influences significantly any carrier interactions.

The interaction of holes with optical phonons is dominated by the deformation potential [6], a mechanism com-

pletely absent for Γ -valley electrons. In contrast to a widespread misconception in literature [3,7,8], the optical deformation potential exclusively couples hole states with *different* orbital symmetry [9,10]. Thus, the rate of HH a ↔ LH b scattering is expected to be much higher than of HH a ↔ HH b (a, b : subband indices). However, first time-resolved experiments for subbands spaced more than the energy of an optical phonon (a situation relevant, e.g., for proposed *p*-type quantum cascade lasers [8]) lack sufficient time resolution [11] and thus give no information on this important issue. Moreover, theoretical predictions for hole scattering rates differ by orders of magnitude [7,8,12], partly due to the neglect of strong orbital symmetry effects on the hole-phonon matrix elements. Here investigation of hole dynamics on the femtosecond time scale and calculations including the matrix effects are required to clarify those issues.

In this Letter, we present a time-resolved study of quasi-two-dimensional hole plasmas, using direct intersubband excitation and probing of heavy holes (HH1 ↔ HH2) in *p*-type modulation-doped Si_{0.5}Ge_{0.5}/Si multiple quantum wells. IS relaxation with a time constant of 250 fs and the subsequent intrasubband carrier heating of holes in the subpicosecond time domain are temporally resolved for the first time. Calculations of optical phonon emission via the deformation potential including wave function symmetries from an eight-band $\mathbf{k} \cdot \mathbf{p}$ model account for the experimental results and reveal that the IS scattering rates originate predominantly from cascaded scattering events between HH- and LH-like subbands.

We study a high-quality *p*-type Si_{0.5}Ge_{0.5}/Si multiple quantum well structure grown by solid-source molecular beam epitaxy [5]. The sample consists of ten periods of Si_{0.5}Ge_{0.5} wells of 4.4-nm width separated by 18-nm thick Si barriers modulation doped with boron ($N_0 = 1.2 \times 10^{12} \text{ cm}^{-2}$). In our time-resolved experiments, holes are excited from the HH1 to the HH2 subband by 150-fs

midinfrared pulses (bandwidth 20 meV) resonant to the optical IS transition shown in Fig. 1(a). Pump and probe pulses at 1 kHz repetition rate are derived from the output of an optical parametric amplifier by difference frequency mixing in a 1-mm thick GaSe crystal [13]. The resulting nonlinear transmission change is monitored as a function of time delay by probe pulses at the same spectral position. After interaction with the sample, the probe pulses are spectrally dispersed in a monochromator (3 meV resolution) and detected by a cooled HgCdTe detector. The coupling to the IS dipole moment is maximized using p -polarized pulses and a prism geometry of the sample. Excitation densities are derived from the pump beam cross section, the sample absorbance, and the pulse energy.

In Fig. 2 we present spectrally resolved data for different time delays between pump and probe. The change of transmission $\Delta T/T_0 = (T - T_0)/T_0$ is plotted versus probe photon energy (dots; T_0 , T : sample transmission

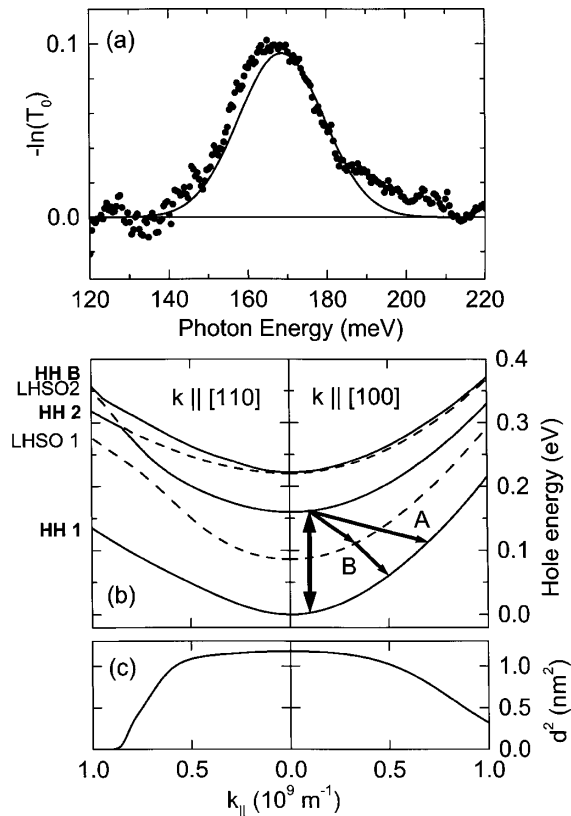


FIG. 1. (a) Dots: stationary intersubband (IS) absorption at 15 K due to $\text{HH1} \leftrightarrow \text{HH2}$ transition (T_0 : sample transmission). Solid line: Calculated absorption spectrum with a homogeneous broadening of 25 meV. (b) Calculated in-plane valence-band dispersion in strained, modulation-doped $\text{Si}_{0.5}\text{Ge}_{0.5}/\text{Si}$ multiple quantum wells (well width 4.4 nm). Femtosecond pulses excite holes from the HH1 to the HH2 subband (vertical arrow). Subsequent IS relaxation occurs predominantly via deformation potential scattering with optical phonons (diagonal arrows: A,B). (c) Calculated dispersion of $\text{HH1} \leftrightarrow \text{HH2}$ squared dipole moment d^2 .

before and after excitation). The excitation density in this measurement was $N_{\text{ex}} = 0.3N_0$ (N_0 : total hole concentration). Directly after excitation, a strong transmission increase (bleaching of IS absorption) occurs around the center of the IS absorption band. At later delay times, a decrease of transmission (enhanced absorption) appears at smaller photon energies.

In Figs. 3(a)–3(c), we show transients at the two characteristic spectral positions (maxima of bleaching and induced absorption) for different excitation densities N_{ex} . At low excitation densities [Figs. 3(a) and 3(b)], both bleaching (positive $\Delta T/T_0$) and enhanced absorption (negative $\Delta T/T_0$) show a delayed rise on a time scale of several 100 fs. The rise of both signals becomes faster with increasing N_{ex} . However, for the highest N_{ex} [Fig. 3(c)], the time evolution of the bleaching changes drastically, displaying a fast rise within the time resolution of the experiment, a maximum at early time delays, and a pronounced decay within the first 2 ps. By contrast, the induced absorption still exhibits the delayed rise (neglecting the coherent artifact due to pump-probe coupling for $\Delta t < 70$ fs

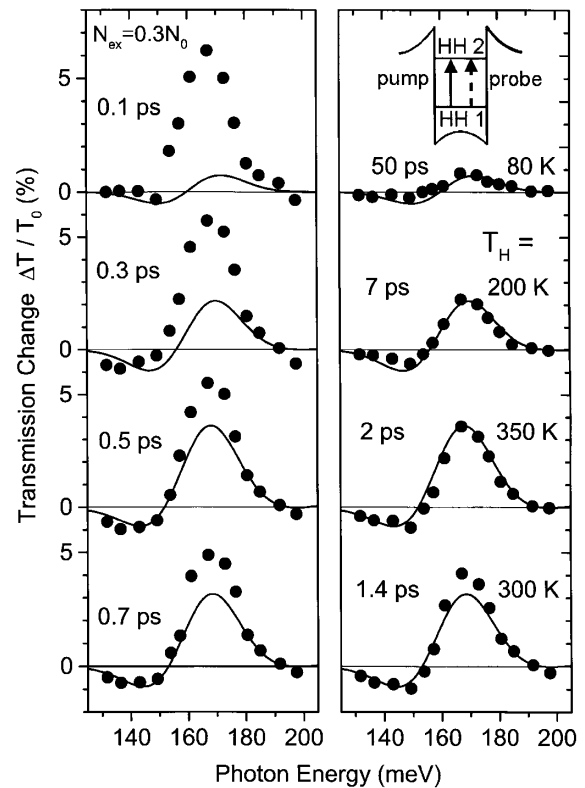


FIG. 2. Dots: Spectrally resolved transmission change at different time delays after femtosecond $\text{HH1} \leftrightarrow \text{HH2}$ IS excitation. Excitation density $N_{\text{ex}} = 0.3N_0$ (doping concentration $N_0 = 1.2 \times 10^{12} \text{ cm}^{-2}$). The transmission change $\Delta T/T_0$ at each fixed temporal delay between pump and probe is plotted versus probe photon energy. Solid lines: calculated difference spectra for thermalized hole distributions for given carrier temperature T_H .

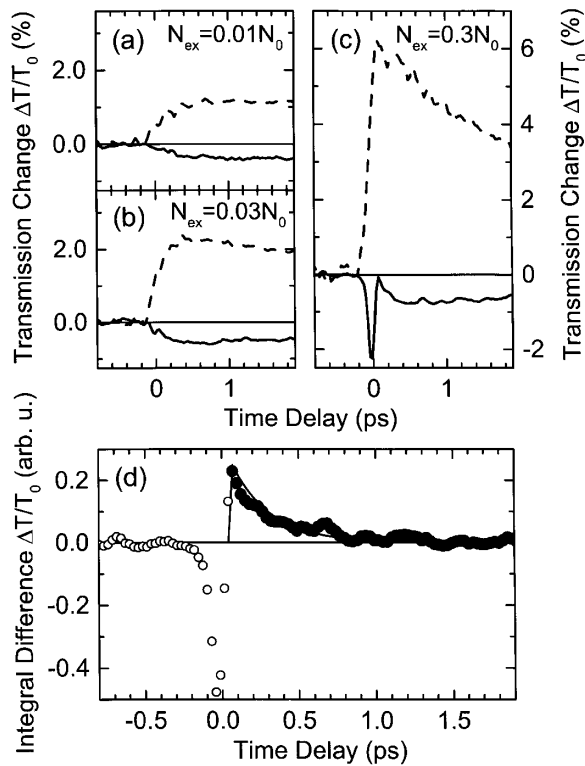


FIG. 3. (a)–(c) Time evolution of nonlinear transmission changes probed at the spectral position of strongest induced bleaching (dashed lines) or strongest enhanced absorption (solid lines). Results are shown for three different excitation densities $N_{\text{ex}}/N_0 =$ (a) 0.01, (b) 0.03, and (c) 0.3. Probe photon energy for maximum bleaching is 168 meV (solid lines), but varies slightly with density to track maximum absorption (dashed lines) at 149, 143, and 140 meV, respectively. (d) Fast bleaching signal obtained from the data, as explained in the text. It reflects IS relaxation in the time range of sequential pump-probe interaction (filled circles, $\Delta t > 70$ fs) [14]. Solid line: Single exponential decay with 250 fs.

[14]), and thus significantly differs from the bleaching dynamics. All transmission changes decay completely on a time scale of 50 to 100 ps (not shown).

We now discuss the valence subband structure of our sample and the nonequilibrium hole dynamics underlying the nonlinear changes of IS absorption. The subband structure was analyzed by an eight-band $\mathbf{k} \cdot \mathbf{p}$ band structure calculation [4] using the parameters of Ref. [5]. Two-dimensional confinement and the $\text{Si}_{0.5}\text{Ge}_{0.5}/\text{Si}$ built-in strain induces a splitting between HH and LH bands and determines the sequence of subbands. In Fig. 1(b), the subbands are plotted for two directions in k_{\parallel} space. They show HH or mixed LH/SO character at $k_{\parallel} = 0$. At low lattice temperatures, the holes present by doping populate only the HH1 subband ($E_{F0} \approx 16$ meV). The calculations yield strong HH1 \rightarrow HH2 IS absorption at 167 meV [arrow, Fig. 1(b)] with a dipole moment oriented normal to the layers, in good agreement with the spectral position of the absorption band measured with p -polarized incident

light [Fig. 1(a)]. In this spectral range, absorption via other IS or intervalence band transitions is negligible. The calculations demonstrate that the dipole moment of the HH1 \rightarrow HH2 IS transition changes strongly with k_{\parallel} [Fig. 1(c)], so that mainly holes close to $k_{\parallel} = 0$ contribute to IS absorption.

Because of the nonparallel in-plane dispersions of the two optically coupled (HH1 and HH2) subbands, the transition energy within the IS absorption line is correlated with the in-plane momentum. Hence, the transmission changes in our time-resolved experiments reflect the transient changes of the hole distributions $\Delta f_n(k_{\parallel}, t) = f_n(k_{\parallel}, t) - f_n^0(k_{\parallel})$ in both optically coupled subbands (n , subband index; f_n^0 , f_n , distribution function before excitation and at time delay t), with $\Delta T(t)/T_0 \propto \Delta f_2(k_{\parallel}, t) - \Delta f_1(k_{\parallel}, t)$ [15]. Specifically, enhanced transmission (bleaching) around the center of the IS absorption line can occur (i) due to stimulated HH2 \rightarrow HH1 emission of holes excited into the HH2 subband, or (ii) due to a depletion of originally occupied HH1 states close to $k_{\parallel} = 0$. In contrast, enhanced absorption in the wings of the IS absorption line stems exclusively from holes in the HH1 subband which transiently populate states at initially unpopulated large in-plane momenta k_{\parallel} .

At low excitation densities, all transients display a delayed rise within several 100 fs [Figs. 3(a) and 3(b)]. Here the depopulation of HH1 states by the excitation pulse and the stimulated emission from holes excited into the HH2 subband play a minor role, as such contributions would rise instantaneously with excitation, in contrast to the experimental findings. Instead, the slow rise of both bleaching and enhanced absorption is governed by *intra*band redistribution processes of carriers in the HH1 subband. During and immediately after the 150 fs excitation pulse, a fraction of holes excited to the HH2 subband undergo IS scattering to high lying states in the HH1 subband. Such holes of high excess energy thermalize with the unexcited holes, forming a hot hole distribution. In this process, holes are transferred from the bottom of the HH1 subband to the high energy tail of the distribution, resulting in the observed decrease of IS absorption around the line center and a concomitant increase at small photon energies. A small fraction of backscattered holes is sufficient to cause a substantial increase of carrier temperature since the heat capacity of the degenerate hole plasma is low. This effect of intra-band redistribution (carrier heating) saturates quickly, yielding a sublinear dependence of the signal on the excitation density. At later times, the signal decays by cooling of the thermalized hole distribution. Data taken at different probe energies demonstrate a similar spectral envelope of $\Delta T/T_0$ at early (heating) and late (cooling) delay times. We conclude that HH1 carriers giving rise to the absorption band form a heated quasiequilibrium distribution even at early delay times.

At the highest excitation density ($N_{\text{ex}} = 0.3N_0$, Fig. 2), the spectra at late delay times ($t \geq 2$ ps) are well

reproduced by calculated difference spectra for quasiequilibrium hole distributions at elevated temperatures T_H (solid lines). At early times [$t < 1.5$ ps, Figs. 2 and 3(c)], however, the spectra display a much stronger bleaching which cannot be reproduced by a hot HH1 distribution. This additional bleaching originates from the initial depletion of HH1 states by the pump pulse and the stimulated emission from HH2 states. The partial decay observed in the bleaching transients is due to depopulation of the HH2 subband and is dominated by the IS relaxation rate [16]. To isolate the IS dynamics, the contribution of HH1 heating at early times has to be subtracted. For this, we use a thermalized HH1 distribution, as suggested by our data for lower excitation density. For each temporal delay, the areas of enhanced absorption and of bleaching were spectrally integrated. The bleaching areas of thermalized spectra ($t \geq 2$ ps) were subtracted from each spectrum with the same area of enhanced absorption, which gives the excess bleaching (filled circles) plotted in Fig. 3(d) as a function of time delay in the range of strictly sequential pump-probe interaction, i.e., for delay times longer than 70 fs [14]. This signal reflects the nonequilibrium population in the HH2 subband, which decays by IS scattering of holes. We derive an IS scattering time of 250 ± 100 fs, much faster than IS scattering of electrons [1].

Now we compare the experimentally observed lifetime of carriers in the HH2 subband with model calculations considering IS scattering of holes by emission of optical phonons via the deformation potential. The correct hole-phonon matrix element $\langle i | \mathbf{D} \cdot \mathbf{u} | f \rangle$ considered here contains hole wave functions $|i\rangle$, $|f\rangle$ of initial and final states from our $\mathbf{k} \cdot \mathbf{p}$ band structure calculation [in the basis of cell-periodic wave functions ($S \uparrow, X \uparrow, Y \uparrow, Z \uparrow, S \downarrow, X \downarrow, Y \downarrow, Z \downarrow$)^T], the wave functions of three-dimensional optical phonons with different polarizations (LO, TO) and corresponding atomic displacements \mathbf{u} [17], and, in contrast to Refs. [3,7,8], the deformation potential tensor \mathbf{D} with correct symmetry (cf. Refs. [9,10]). Each phonon polarization component couples to different types of valence band states; for example, the basis functions $|X \uparrow\rangle$ and $|Y \uparrow\rangle$ are coupled when both fcc sublattices are displaced relative to each other in the z direction. After summation over the final states (Fermi's golden rule), for an optical deformation potential constant of $d_O = 36$ eV [6] and a lattice temperature $T = 15$ K, we obtain scattering times of $\tau_{\text{HH2} \rightarrow \text{HH1}} = 760$ fs, $\tau_{\text{HH2} \rightarrow \text{LH SO1}} = 319$ fs, and $\tau_{\text{LH SO1} \rightarrow \text{HH1}} = 170$ fs. This yields an overall HH2 depopulation time of 225 fs, which is in good agreement with the measured IS scattering time. It is important to note that due to the symmetry of the deformation potential tensor the cascaded indirect process via the LH SO1 subband [arrow *B* in Fig. 1(b)] is about 3 times faster than

direct $\text{HH2} \leftrightarrow \text{HH1}$ intersubband scattering (arrow *A*), in contrast to the interpretation given in Ref. [3].

In conclusion, we have presented the first femtosecond study of the hole relaxation after resonant intersubband excitation in a quasi-two-dimensional semiconductor. The midinfrared pump-probe studies on p -type $\text{Si}_{0.5}\text{Ge}_{0.5}/\text{Si}$ multiple quantum wells reveal an intersubband relaxation time of 250 fs from the second heavy-hole back to the first heavy-hole subband, in good agreement with calculations considering cascaded emission of optical phonons via the deformation potential interaction. The strong reshaping of the intersubband absorption line experimentally observed during relaxation is accounted for by detailed calculations of the subband structure and the optical spectra.

-
- [1] For a review see T. Elsaesser and M. Woerner, Phys. Rep. **321**, 253 (1999).
 - [2] J. Faist *et al.*, Science **264**, 553 (1994).
 - [3] Z. Xu *et al.*, Phys. Rev. B **51**, 10 631 (1995).
 - [4] D. Gershoni *et al.*, IEEE J. Quantum Electron. **29**, 2433 (1993).
 - [5] T. Fromherz *et al.*, Phys. Rev. B **50**, 15 073 (1994).
 - [6] W. Poetz and P. Vogl, Phys. Rev. B **24**, 2025 (1981).
 - [7] K. Bhaumik *et al.*, J. Appl. Phys. **74**, 5546 (1993).
 - [8] L. Friedman, R. A. Soref, and G. Sun, J. Appl. Phys. **83**, 3480 (1998).
 - [9] M. Woerner and T. Elsaesser, Phys. Rev. B **51**, 17 490 (1995).
 - [10] R. Scholz, J. Appl. Phys. **77**, 3219 (1995).
 - [11] P. Boucaud *et al.*, Appl. Phys. Lett. **69**, 3069 (1996).
 - [12] P. Lautenschlager, P. B. Allen, and M. Cardona, Phys. Rev. B **33**, 5501 (1986).
 - [13] R. A. Kaindl *et al.*, J. Opt. Soc. Am. B **17**, 2086 (2000).
 - [14] Components from different interaction sequences of pump and probe fields can contribute to pseudo-two-color pump-probe signals [see, e.g., M. Chachisvilis *et al.*, Chem. Phys. Lett. **234**, 141 (1995)]: (i) perturbed free induction decay, (ii) coherent pump-probe coupling, and (iii) strictly sequential pump-probe interaction. Whereas (i) and (ii) contribute only at negative delay times and during pump-probe overlap [$\Delta t < 70$ fs], the population difference is reflected by (iii) [$\Delta t \geq 70$ fs].
 - [15] Many-body calculations using the local-density approach reported by M. Zaluzny [Phys. Rev. B **49**, 2923 (1994)] show that many-body effects have a negligible influence on the shape of absorption changes observed here. Thus, a single-particle picture is appropriate.
 - [16] Population changes of optically coupled states in the HH1 subband would give rise to an *increase* of the bleaching component by heating of the HH1 hole plasma; i.e., they cannot account for this decay.
 - [17] The optical phonon spectrum in strained SiGe/Si quantum wells consists of Si-Si ($\hbar\omega = 61$ meV), Si-Ge (50 meV), and Ge-Ge (36 meV) oscillations [7].